

Event Structure at RHIC from p-p to Au-Au

Thomas A. Trainor¹ (STAR Collaboration)

¹CENPA 354290, University of Washington,
Seattle, USA

Abstract. Several correlation analysis techniques are applied to p-p and Au-Au collisions at RHIC. Strong large-momentum-scale correlations are observed which can be related to local charge and momentum conservation during hadronization and to minijet (minimum-bias parton fragment) correlations.

Keywords: heavy ions, correlations, fluctuations, minijets, hadronization
PACS: 25.75.Gz, 24.60.Ky

1. Introduction

Two-particle momentum distributions from p-p and Au-Au collisions are projected onto subspaces ($y_t \otimes y_t$) and ($\eta_\Delta \otimes \phi_\Delta$) for charge-independent (CI or isoscalar) and charge-dependent (CD or isovector) charge combinations, revealing strong correlations related to parton dynamics, a color medium and changes in hadronization.

2. p-p Collisions: The Essential A-A Reference

The structure of hadron distributions from p-p collisions provides an essential reference for A-A collisions. Normalized p_t distributions for several event multiplicity classes of p-p collisions from RHIC at $\sqrt{s} = 200$ GeV [1] shown in Fig. 1 (left panel) can be decomposed into a soft component and a semi-hard or minijet component. p-p event multiplicity at this energy determines the frequency of hard scatters in each event class. A two-component model function is used to describe the data: $1/p_t dN/dp_t = n_s(n_{ch}) S_0(p_t) + n_h(n_{ch}) H_0(p_t)$, with soft and hard reference components $S_0(p_t)$ and $H_0(p_t)$ (independent of n_{ch} by hypothesis) both integrating to unity on p_t . Transforming to transverse rapidity $y_t \equiv \ln\{(m_t + p_t)/m_0\}$ as a velocity variable provides a ‘native’ description of minijets as hadron fragments from a moving source. We observe in Fig. 1 that soft-component S_0 (dash-dot curve, string fragments) is well represented on transverse rapidity y_t by an error function (corresponding to a Lévy or ‘power-law’ distribution on m_t), and hard component

H_0 (dashed curve, minijet fragments) is represented by a gaussian distribution on y_t , each form approximately independent of event multiplicity and determined by two parameters. The stability of the minijet fragment distribution with event multiplicity (right panel = center-panel $- S_0(y_t)$) shows that gaussian distribution H_0 on y_t is a good minimum-bias minijet input for A-A collision models.

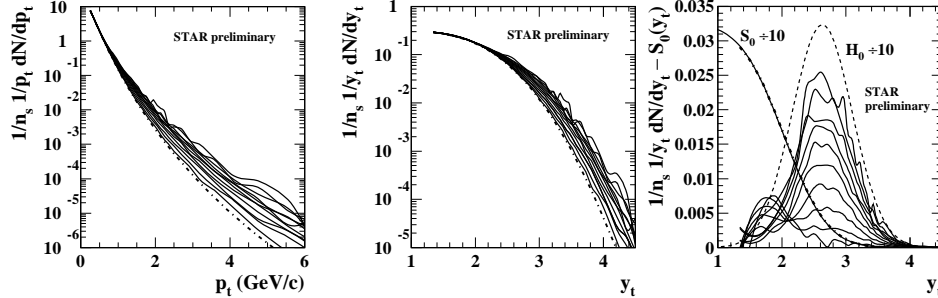


Fig. 1. Panels from left to right: inclusive p_t distributions for $n_{ch} \in [1, 12]$, same on transverse rapidity y_t , soft reference S_0 subtracted to reveal hard components.

We have also measured p-p two-particle correlations [2] on transverse momentum p_t ($0.15 \leq p_t \leq 6.0$ GeV/c) transformed to transverse rapidity y_t . We observe large-scale correlation structures also consistent with p-p collisions having soft (string) and semi-hard (minijet) components. Fig. 2 (left panel) shows correlation function $C(y_{t1}, y_{t2}) = \rho_{sibling} - \rho_{mix}$ for STAR data. At low y_t a soft component (string fragments) falls rapidly with increasing y_t . At higher y_t the structure is centered around $y_{t1} = y_{t2} \simeq 2.6$ ($p_{t1} = p_{t2} \simeq 1.0$ GeV/c) and attributed to correlated fragments from semi-hard parton scatters (*cf* distributions in Fig. 1 (right panel)).

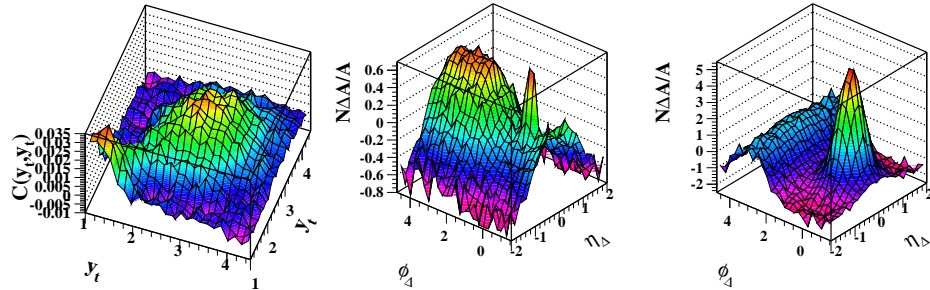


Fig. 2. $y_t \otimes y_t$ correlations (left) and $\eta_{\Delta} \otimes \phi_{\Delta}$ correlations for the soft component (center) and hard component (right) of the $y_t \otimes y_t$ correlations.

These $y_t \otimes y_t$ correlations provide a cut space for analysis of axial momentum correlations [2]. We construct joint autocorrelations on axial *difference variables* $\eta_{\Delta} \equiv \eta_1 - \eta_2$ (pseudorapidity) and $\phi_{\Delta} \equiv \phi_1 - \phi_2$ (azimuth angle) as pair-number ratio histograms. The right two panels in Fig. 2 show autocorrelations from two y_t

selections in the left panel. The center panel (soft component) shows a broad peak on η_Δ caused by local charge conservation (charge ordering) on the fragmenting string. The depression on ϕ_Δ near zero represents local transverse momentum conservation. The narrow peak is conversion electron pairs. The right panel (hard component) shows a near-side peak symmetric about $\eta_\Delta = \phi_\Delta = 0$ and a broad η_Δ -independent away-side ridge. The near-side peak represents fragments distributed about a common jet thrust axis, and the away-side ridge correlates particles between opposing jets. Persistence of those structures to low hadron p_t (~ 0.5 GeV) may indicate that *minimum-bias* partons down to $p_t \sim 1$ GeV fragment to ‘minijets’ of one or a few hadrons.

3. $\langle p_t \rangle$ Fluctuations and p_t Correlations in Au-Au

The scale (bin-size) dependence of event-wise mean transverse momentum $\langle p_t \rangle$ fluctuations [3] can be inverted [4] to obtain joint p_t autocorrelations on pseudo-rapidity and azimuth angle difference variables representing velocity/temperature correlations. The structure and centrality dependence of those components suggest that the principal origin is minijets, altered by a dissipative color medium in the more central Au-Au collisions. Difference factor $\Delta\sigma_{p_t:n}$ is related to a *variance-*

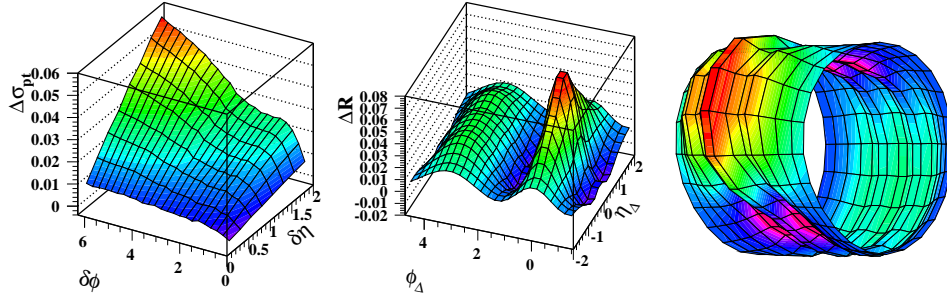


Fig. 3. Fluctuation scale dependence, inversion to p_t autocorrelation and same autocorrelation distribution in cylindrical format.

difference measure of nonstatistical p_t fluctuations by $\Delta\sigma_{p_t:n}^2 \equiv 2\sigma_{\hat{p}_t}\Delta\sigma_{p_t:n}$. The variance difference is related to joint p_t autocorrelation ΔR by integral equation

$$\Delta\sigma_{p_t:n}^2(m\epsilon_\eta, n\epsilon_\phi) \equiv 4\hat{p}_t^2 \sum_{k,l=1}^{m,n} \epsilon_\eta\epsilon_\phi K_{mn;kl} \Delta R_{kl}(p_t : n; \epsilon_\eta, \epsilon_\phi). \quad (1)$$

In Fig. 3 (left panel) is the variation with bin sizes ($\delta\eta, \delta\phi$) of $\langle p_t \rangle$ fluctuation measure $\Delta\sigma_{p_t:n}$ for central Au-Au collisions at $\sqrt{s_{NN}} = 200$ GeV up to the limiting STAR acceptance. The 2D joint autocorrelation on difference variables (center panel) obtained by inverting Eq. (1) has a near-side peak and away-side ridge which depend separately and strongly on collision centrality, and can be compared with

Figs. 2 (right panel) and 4 (left panels). The same distribution in cylindrical format (right panel) reveals ‘necking’ on azimuth difference variable ϕ_Δ . This autocorrelation summarizes the complex velocity/temperature structure of multiple minijets and the bulk medium in each collision, averaged over many central Au-Au collisions.

4. Parton Deformation in Au-Au Collisions

Charge-independent (CI) joint number autocorrelations on difference variables η_Δ and ϕ_Δ were measured for particles with $0.15 \leq p_t \leq 2$ GeV/ c from Au-Au collisions at $\sqrt{s_{NN}} = 130$ GeV [5]. In Fig. 4 (left panels) are autocorrelations for peripheral (d) and central (a) collisions with multipole components representing elliptic flow (v_2) and momentum conservation (v_1) removed, revealing minijet fragment angular distributions (conversion-electron pairs contribute to (0,0) bins). The (η, ϕ) minijet angular correlations, symmetric about the origin in p-p and peripheral HI collisions (d), are strongly deformed in central collisions (a). Joint autocorrelations were fitted with a model function including azimuthal dipole and quadrupole terms and a 2D gaussian. Fitted gaussian widths σ_η and σ_ϕ (right panel) *vs* centrality measure ν (mean participant path length as number of encountered nucleons) show a dramatic centrality dependence. Minijet peak structure varies in angular shape with

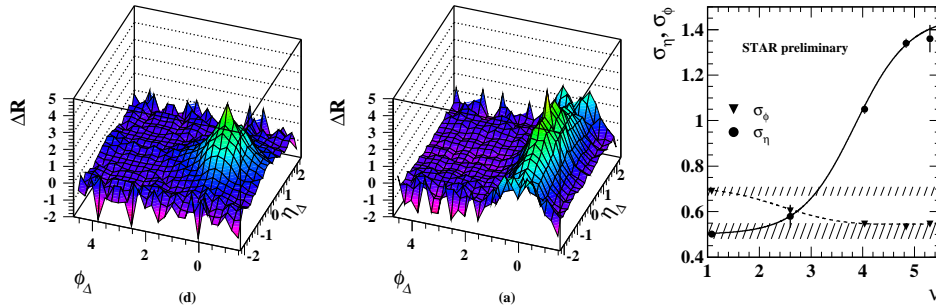


Fig. 4. Joint number autocorrelations with multipoles removed for peripheral (d) and central (a) events, and minijet width parameters *vs* centrality ν .

centrality from a symmetric shape on $(\eta_\Delta, \phi_\Delta)$ for peripheral collisions to a highly asymmetric peak for central collisions. This trend can be interpreted as a transition from *in vacuo* parton fragmentation similar to p-p collisions in peripheral heavy ion collisions to strong coupling of minimum-bias partons to a longitudinally-expanding color medium in central collisions. This result is inconsistent with pQCD-based models of jet quenching but may favor some recombination models.

5. Centrality Evolution of Hadronization Geometry

Charge-dependent (CD) joint number autocorrelations on difference variables η_Δ and ϕ_Δ were measured for primary charged hadrons with $0.15 \leq p_t \leq 2$ GeV/ c from Au-Au collisions at $\sqrt{s_{NN}} = 130$ GeV [5]. Large-scale correlation structures, not predicted by theory, are consistent with a change in the geometry of hadron emission with increasing centrality of Au-Au collisions. In p-p collisions charge-dependent correlations are dominated by a 1D gaussian on η_Δ indicative of charge-ordering on the axial string as shown shown by 200 GeV p-p data in Fig. 5 (left panel) [2]. In central Au-Au collisions CD correlations are dominated by a peak at (0,0) nearly exponential in shape and nearly symmetric on (η, ϕ) . Fig. 5 (center panel) shows CD correlations for the most central event class in this study: the 1D gaussian peak on η_Δ has disappeared and the amplitude of the central 2D exponential peak is eight times as large. Joint autocorrelations for four centrality classes were fitted with a model consisting of a 2D exponential with independent widths on η_Δ and ϕ_Δ , and a 1D gaussian on η_Δ . Fitted width parameters are shown (right panel) *vs* centrality measure ν . These data are consistent with local

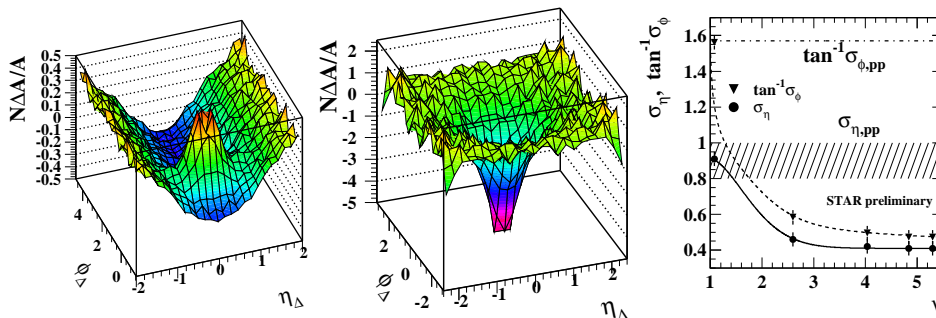


Fig. 5. Charge-dependent number autocorrelations for p-p collisions, central Au-Au collisions, and width parameters *vs* centrality measure ν .

charge conservation or canonical suppression of net charge fluctuations. The strong variation of correlation structure from p-p to peripheral Au-Au to central Au-Au can be interpreted as follows: Hadronization geometry evolves from 1D color-string fragmentation in p-p collisions to exponentially-attenuated 2D charge-ordered emission from a hadron-opaque medium in central Au-Au collisions. These results are qualitatively inconsistent with standard HI collision models and predictions of QGP-related strong suppression of net-charge fluctuations.

6. Energy Dependence of $\langle p_t \rangle$ Fluctuations

Controversy has emerged over the $\sqrt{s_{NN}}$ dependence of $\langle p_t \rangle$ fluctuations in heavy ion collisions from SPS to RHIC energies. Analysis of p_t autocorrelations (*cf* Sec. 3)

at 20 and 200 GeV indicates a strong and monotonic increase with collision energy, with nontrivial $\langle p_t \rangle$ fluctuations first appearing at a threshold of observability near 10 GeV. Analysis based on ‘temperature fluctuations’ on the other hand [6] suggests that $\langle p_t \rangle$ fluctuations are nearly independent of collision energy over this interval. In Fig. 6 (left two panels) is a comparison of *per particle* p_t autocorrelations inferred from STAR $\langle p_t \rangle$ fluctuation scale dependence at 20 and 200 GeV [3], with the same detector and analysis system in each case. A dramatic difference in fluctuations/correlations between SPS (~ 20 GeV) and RHIC (~ 200 GeV) energies is evident. The right-most panel shows the trend on collision energy (12.6, 17.8, 20 130 and 200 GeV) of the large-scale correlation (LSC) component of p_t autocorrelations projected onto difference variable η_Δ . This projection permits direct comparison with CERES’ measurements of $\Phi_{p_t}(\delta\eta) \approx \Delta\sigma_{p_t:n}(\delta\eta)$ variation with pseudorapidity bin size [6]. LSC, defined as the autocorrelation amplitude at *large* η_Δ , is distinguished from small-scale correlations (SSC), which especially at SPS energies are dominated by quantum (HBT) and Coulomb correlations. We observe that the principal mechanism for $\langle p_t \rangle$ fluctuations at RHIC is minijets. The energy dependence of the LSC component is therefore of considerable interest: what is the energy trend of semi-hard parton scattering, as manifested by correlated hadron fragments, down to the lowest relevant collision energy?

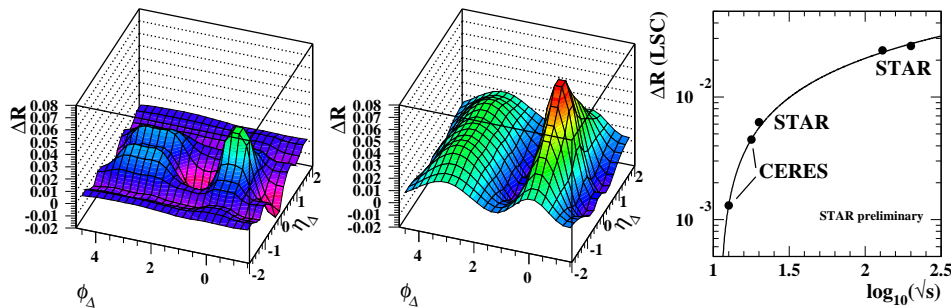


Fig. 6. STAR p_t autocorrelations at 20 and 200 GeV, and energy dependence of large-scale correlations (LSC) from SPS to RHIC energies.

7. Conclusions

By comparing correlation structures in p-p and Au-Au collisions obtained by several analysis methods we gain important new information about the changing geometry of hadronization and the interaction of low- p_t or minimum-bias partons with the colored medium generated in the more central Au-Au collisions. We find that minimum-bias partons are sensitive to the velocity structure of the medium, and the hadronization process is dramatically different from that in elementary collisions.

References

1. T. A. Trainor (STAR Collaboration), Bull. Am. Phys. Soc. **48**, 25 (2003).
2. R. J. Porter (STAR Collaboration), Bull. Am. Phys. Soc. **48**, 25 (2003).
3. T. A. Trainor (STAR Collaboration), Bull. Am. Phys. Soc. **48**, 25 (2003).
4. D. J. Prindle (STAR Collaboration), Bull. Am. Phys. Soc. **48**, 25 (2003).
5. A. Ishihara (STAR Collaboration), Bull. Am. Phys. Soc. **48**, 25 (2003).
6. D. Adamova *et al.* (CERES Collaboration), Nucl. Phys. A **727**, 97 (2003).